

REPORT DOCUMENTATION PAGE			Form Approved OMB NO. 0704-0188		
<p>The public reporting burden for this collection of information is estimated to average 1 hour per response, including the time for reviewing instructions, searching existing data sources, gathering and maintaining the data needed, and completing and reviewing the collection of information. Send comments regarding this burden estimate or any other aspect of this collection of information, including suggestions for reducing this burden, to Washington Headquarters Services, Directorate for Information Operations and Reports, 1215 Jefferson Davis Highway, Suite 1204, Arlington VA, 22202-4302. Respondents should be aware that notwithstanding any other provision of law, no person shall be subject to any penalty for failing to comply with a collection of information if it does not display a currently valid OMB control number.</p> <p>PLEASE DO NOT RETURN YOUR FORM TO THE ABOVE ADDRESS.</p>					
1. REPORT DATE (DD-MM-YYYY) 03-02-2013		2. REPORT TYPE Final Report		3. DATES COVERED (From - To) 1-Aug-2007 - 31-Oct-2012	
4. TITLE AND SUBTITLE Selective Capture of CWAs and Containment of Their Neutralization Byproducts by Porous Frameworks Presenting Self-Amplifying and Self-Regulating Reactivities			5a. CONTRACT NUMBER W911NF-07-1-0533		
			5b. GRANT NUMBER		
			5c. PROGRAM ELEMENT NUMBER BD2231		
6. AUTHORS Dongwhan Lee, Omar M. Yaghi			5d. PROJECT NUMBER		
			5e. TASK NUMBER		
			5f. WORK UNIT NUMBER		
7. PERFORMING ORGANIZATION NAMES AND ADDRESSES Indiana University at Bloomington Trustees of Indiana University 509 E 3RD ST Bloomington, IN 47401 -3654			8. PERFORMING ORGANIZATION REPORT NUMBER		
9. SPONSORING/MONITORING AGENCY NAME(S) AND ADDRESS(ES) U.S. Army Research Office P.O. Box 12211 Research Triangle Park, NC 27709-2211			10. SPONSOR/MONITOR'S ACRONYM(S) ARO		
			11. SPONSOR/MONITOR'S REPORT NUMBER(S) 53438-CH.6		
12. DISTRIBUTION AVAILABILITY STATEMENT Approved for Public Release; Distribution Unlimited					
13. SUPPLEMENTARY NOTES The views, opinions and/or findings contained in this report are those of the author(s) and should not be construed as an official Department of the Army position, policy or decision, unless so designated by other documentation.					
14. ABSTRACT We have designed and synthesized highly porous COFs and MOFs as functional architectures that are capable of capturing volatile TICs. In parallel, we have explored novel crystalline porous materials that have reactive sites and functionalities, which can be controlled by an external stimulus. We demonstrated that reticular chemistry facilitates the design and synthesis of new robust COFs, as well as isorecticular covalent functionalization and metallation. In addition, a MOF with self-contained photo-active switches was prepared. As stimuli-responsive					
15. SUBJECT TERMS covalent organic frameworks, metal-organic frameworks, toxic industrial chemicals, volatile organic chemicals, chemical warfare agents, adsorption					
16. SECURITY CLASSIFICATION OF:		17. LIMITATION OF ABSTRACT		15. NUMBER OF PAGES	
a. REPORT UU	b. ABSTRACT UU	c. THIS PAGE UU	UU	19a. NAME OF RESPONSIBLE PERSON Dongwhan Lee	
				19b. TELEPHONE NUMBER 812-856-9364	

Report Title

Selective Capture of CWAs and Containment of Their Neutralization Byproducts by Porous Frameworks Presenting Self-Amplifying and Self-Regulating Reactivities

ABSTRACT

We have designed and synthesized highly porous COFs and MOFs as functional architectures that are capable of capturing volatile TICs. In parallel, we have explored novel crystalline porous materials that have reactive sites and functionalities, which can be controlled by an external stimulus. We demonstrated that reticular chemistry facilitates the design and synthesis of new robust COFs, as well as isorecticular covalent functionalization and metallation. In addition, a MOF with self-contained photo-active switches was prepared. As stimuli-responsive functional molecules that can release multiple copies of nucleophilic agents to combat electrophilic CWAs, we have developed linear/branched oligoether/esters. Upon cleavage of a Si–O bond, fast and repetitive QM rearrangement occur along the molecular backbone to release phenoxide derivatives that detoxify OP agent simulant. The progress of such reaction could be visually monitored by a large enhancement in the fluorescence intensity, which allows for detection and detoxification achieved by a single integrated molecular system. These functional modules could be grafted onto chemically modified inorganic surfaces. Shape-persistent conducting polymers were also prepared from borasiloxane cage molecules. The light-absorbing properties and electrical conductivities of these materials change in a reversible fashion upon exposure to volatile TICs.

Enter List of papers submitted or published that acknowledge ARO support from the start of the project to the date of this printing. List the papers, including journal references, in the following categories:

(a) Papers published in peer-reviewed journals (N/A for none)

<u>Received</u>	<u>Paper</u>
01/31/2013	2.00 William Morris, Christian J. Doonan, Omar M. Yaghi. Postsynthetic Modification of a Metal–Organic Framework for Stabilization of a Hemiaminal and Ammonia Uptake, <i>Inorganic Chemistry</i> , (08 2011): 0. doi: 10.1021/ic200744y
01/31/2013	3.00 Hexiang Deng, Mark A. Olson, J. Fraser Stoddart, Omar M. Yaghi. Robust dynamics, <i>Nature Chemistry</i> , (05 2010): 0. doi: 10.1038/nchem.654
01/31/2013	4.00 Omar M. Yaghi, Qiaowei Li. Reticular Chemistry and Metal-Organic Frameworks for Clean Energy, <i>MRS Bulletin</i> , (01 2011): 0. doi: 10.1557/mrs2009.180
01/31/2013	5.00 Joseph R. Hunt, Christian J. Doonan, James D. LeVangie, Adrien P. Co?te?, Omar M. Yaghi. Reticular Synthesis of Covalent Organic Borosilicate Frameworks, <i>Journal of the American Chemical Society</i> , (09 2008): 0. doi: 10.1021/ja805064f
TOTAL:	4

Number of Papers published in peer-reviewed journals:

(b) Papers published in non-peer-reviewed journals (N/A for none)

Received

Paper

TOTAL:

Number of Papers published in non peer-reviewed journals:

(c) Presentations

D. Britt, D. Tranchemontagne, O. M. Yaghi, Metal-organic frameworks for air purification. IPE 2007, October 2007, Melbourne, Australia.

D. Britt, Challenges in the application of metal-organic frameworks to air purification, the Advanced Filtration Workshop, September 2009, Arlington, VA.

O. M. Yaghi, Chemistry and porosity of metal-organic frameworks, Seminar in the Dept. of Chemistry, UC Berkeley, October 2009, Berkeley, CA.

O. M. Yaghi, Reticular chemistry where geometry becomes beautifully real and useful, ACS Southern Regional Meeting, October 2009, San Juan, Puerto Rico.

O. M. Yaghi, Porous crystals as molecules, Eleventh International Conference on Organic Chem., November 2009, Kyoto, Japan (Plenary talk).

D. Britt, Controlled post-synthesis incorporation of accessible metal sites in a metal-organic framework, the 2009 Chemical and Biological Defense Science and Technology (CBD S&T) Conference, November 2009, Dallas, TX.

O. M. Yaghi, Metal-organic frameworks and their applications to clean energy, 5th Intl. Symposium on Macrocyclic and Supramolecular Chemistry, June 2010, Nara, Japan (Plenary talk).

O. M. Yaghi, Zeolitic imidazolate frameworks, 5th International Zeolite Membrane Meeting, May 2010, Loutraki, Greece (Plenary talk).

O. M. Yaghi, Reticular chemistry and its applications to clean energy, Seminar in University of Milan, May 2010, Italy.

O. M. Yaghi, Frontiers in materials chemistry, 239th ACS National Meeting & Exposition, March 2010, San Francisco, CA (Plenary talk).

H. Furukawa, Inclusion of reactive sites within metal-organic frameworks: synthesis and characterization, the Advanced Filtration Workshop, September 2010, Arlington, VA.

O. M. Yaghi, Metal-organic frameworks and their applications to clean energy, Welch Conference on Green Chemistry and Sustainable Energy, October 2010, Houston, TX.

O. M. Yaghi, Metal-organic frameworks and their applications to clean energy, 1st United Arab Emirates Conference on Pure and Applied Chemistry (ECPAC11), March 2011, Sharjah, UAE.

O. M. Yaghi, Perspectives on MOF research and the UCLA center for global mentoring, VNUHCM-UCLA Symposium: Chemistry of MOFs and Related Materials, March 2011, Ho Chi Minh City, Vietnam.

O. M. Yaghi, Metal-organic frameworks and their applications to carbon capture, 8th U.S.-Korea Forum on Nanotechnology, April 2011, Pasadena, CA.

O. M. Yaghi, The 'Gene' Within Metal-Organic Frameworks, Eyring Lectures in Chemistry & Biochemistry, April 2011, Arizona State University, Tempe, AZ.

O. M. Yaghi, Metal-organic frameworks and their applications to clean energy, Saudi International Petrochemicals Technologies Conference 2011, June 2011, KACST, Saudi Arabia.

W. Morris, H. Furukawa, S. Demir, B. Voloskiy, M. Hmadeh, O. M. Yaghi, Zirconium based metal organic frameworks (MOFs) with high chemical stability and variable pore metrics for filter applications, the 2011 Chemical and Biological Defense Science and Technology (CBD S&T) Conference, November 2011, Las Vegas, NV.

H. Furukawa, Inclusion of reactive sites within metal-organic frameworks, the Advanced Filtration Workshop, August 2012, Arlington, VA.

Dongwhan Lee, Targeting and Triggering Basic Research Workshop (co-organized by ARO and DSTL), Cambridge, UK (May 14–16, 2012).

Dongwhan Lee, 240th ACS National Meeting, Boston, MA (Aug 23, 2010): Symposium “From Molecules to Macromolecules: Toward Self-Assembling Materials”

Dongwhan Lee, NBIC Transdisciplinary Strategic Science Workshop (June 29, 2009), Naval Research Laboratory, Washington, DC.

Dongwhan Lee, Physical Organic Chemistry NSF Workshop (September 14–18, 2008), Lake Tahoe, CA.

“Investigating the Reactive Landscape of Porous Materials”, Opsitnick, E. A.; Lee, H. Y.; Jiang, X.; Lee, D. 42th Meeting of the ACS Central Region, Indianapolis, IN, June 8–10, 2011.

“Fluorescent Probes for Cyanide Detection in Water: Reactivity-Based Chemical Sensing Scheme with Peptide β -Turn Mimic”, Lee, D. 2010 Chemical and Biological Defense (CBD) Science and Technology Conference, Orlando, FL, November 15–19, 2010.

“C3-Symmetric conjugation supported by tris(hydrazone) platform: Elucidation of tautomeric state and application to amine vapor sensing”, Lee, H. Y.; Song, X.; Park, H.; Lee, D. 240th ACS National Meeting, Boston, MA, August 22–26, 2010.

“Electroactive cages and their linear conjugates: Inorganic–organic hybrid platforms for chemical sensing and charge transport”, Lee, D., 240th ACS National Meeting, Boston, MA, August 22–26, 2010.

“Mechanism-based design of fluorescent molecular probes: A biomimetic approach to turn-on detection of cyanide ion in water”, Jo, J.; Lee, D. 239th ACS National Meeting, San Francisco, CA, March 21–25, 2010.

“Borasiloxane-Derived Conjugated Polymer Sensors for Naked-Eye Detection of Toxic Volatile Chemicals”, Liu, W.; Pink, M.; Lee, D. Chemical and Biological Defense (CBD) Physical Science and Technology Conference, Dallas, TX, November 16–20, 2009.

“Conjugated polymer sensors built with borasiloxane cage molecules: Reversible control of optoelectronic properties through Lewis acid–base interactions”, Liu, W.; Pink, M.; Lee, D. 238th ACS National Meeting, Washington, DC, August 16–20, 2009.

“Toward self-amplifying and self-regulating modules for CWA detection and neutralization: Controlled chain fragmentation of surface-bound dendritic sensors, Lee, H. Y.; Jiang, X.; Lee, D. Chemical and Biological Defense (CBD) Physical Science and Technology Conference, New Orleans, LA, November 17–21, 2008.

The following peer-reviewed publications (from the PI Dongwhan Lee's group) could not be uploaded due to technical problems at ARO Extranet during submission.

[1] Riddle, J. A.; Jiang, X.; Lee, D. Conformational dynamics for chemical sensing: simplicity and diversity. *Analyst*, 2008, 133, 417–422.

[2] Lee, H. Y.; Jiang, X.; Lee, D. Kinetics of Self-Immolation: Faster Signal Relay over a Longer Linear Distance? *Org. Lett.* 2009, 11, 2065–2068.

[3] Liu, W.; Pink, M.; Lee, D. Conjugated Polymer Sensors Built on π -Extended Borasiloxane Cages. *J. Am. Chem. Soc.* 2009, 131, 8703–8707.

[4] Jo, J.; Lee, D. Turn-On Fluorescence Detection of Cyanide in Water: Activation of Latent Fluorophores through Remote Hydrogen Bonds That Mimic Peptide β -Turn Motif. *J. Am. Chem. Soc.* 2009, 131, 16283–16291.

[5] Lee, H.; Song, X.; Park, H.; Baik, M.-H.; Lee, D. Torsionally Responsive C3-Symmetric Azo Dyes: Azo–Hydrazone Tautomerism, Conformational Switching, and Application for Chemical Sensing. *J. Am. Chem. Soc.* 2010, 132, 12133–12144.

[6] Lee, H. Y.; Jo, J.; Park, H.; Lee, D. Ratiometric detection of mercury ion in water: accelerated response kinetics of azo chromophores having ethynyl ligand tethers. *Chem. Commun.* 2011, 47, 5515–5517.

[7] Hutt, J. T.; Jo, J.; Olasz, A.; Chen, C.-H.; Lee, D.; Aron, Z. D. Fluorescence Switching of Imidazo[1,5-a]pyridinium Ions: pH-Sensors with Dual Emission Pathways. *Org. Lett.* 2012, 14, 3162–3165.

[8] Lee, H. Y.; Olasz, A.; Chen, C.-H.; Lee, D. Three-Stage Binary Switching of Azoaromatic Polybase. *Org. Lett.* 2012, 14, 6286–6289.

[9] Jo, J.; Lee, H. Y.; Liu, W.; Olasz, A.; Chen, C.-H.; Lee, D. Reactivity-Based Detection of Copper(II) Ion in Water: Oxidative Cyclization of Azoaromatics as Fluorescence Turn-On Signaling Mechanism. *J. Am. Chem. Soc.* 2012, 134, 16000–16007.

Number of Presentations: 31.00

Non Peer-Reviewed Conference Proceeding publications (other than abstracts):

Received Paper

TOTAL:

Number of Non Peer-Reviewed Conference Proceeding publications (other than abstracts):

Peer-Reviewed Conference Proceeding publications (other than abstracts):

Received Paper

TOTAL:

Number of Peer-Reviewed Conference Proceeding publications (other than abstracts):

(d) Manuscripts

Received Paper

06/04/2008 1.00 Justin Riddle, Xuan Jiang, Dongwhan Lee. Conformational Dynamics for Chemical Sensing: Simplicity and Diversity,
()

TOTAL: 1

Number of Manuscripts:

Books

Received

Paper

TOTAL:

Patents Submitted

US Patent Application, 20120133939

~~O. M. Yaghi, D. K. Britt, B. Wang, Carbon dioxide capture and storage using open frameworks~~

Patents Awarded

Awards

Honors and Awards to Omar Yaghi:

2011 TOP 2 most cited chemist worldwide (ISI Thomson)

2011 Distinguished Professor, Vietnam National University, Vietnam

2011 Icon Professor, University of Malaya, Malaysia

2010 Royal Society of Chemistry Centenary Prize

2009 World Class Professor, KAIST, Korea

2009 Izatt-Christensen International Award in Macrocyclic Chemistry

2009 American Chemical Society, ACS Award in the Chemistry of Materials

2009 Musher Lectureship, Hebrew University, Israel

2009 The Gooch-Stephens Lectures, Baylor University

2009 Miller Visiting Professorship at University of California-Berkeley

2008 AAAS Newcomb Cleveland Prize for the most outstanding paper in Science

2008 US National Science Foundation Distinguished Lecturer

2008 Guggenheim Lectureship, Reading University, UK

2008 G. Schmidt Lectureship, Weizmann Institute, Israel

2007 Materials Research Society, MRS Medal Sole Recipient

2007 Deans Recognition Award, UCLA

Honors and Awards to Dongwhan Lee:

2008–2010 Alfred P. Sloan Research Fellowship

Graduate Students

<u>NAME</u>	<u>PERCENT SUPPORTED</u>	<u>Discipline</u>
William Morris	0.04	
Joseph Hunt	0.10	
Qiaowei Li	0.10	
Peter Klonowski	0.03	
Guannan Liu	0.02	
James LeVangie	0.02	
Anh Phan	0.02	
Junyong Jo	0.05	
Byung Gyu Park	0.05	
Elizabeth Opsitnick	0.10	
Wenjun Liu	0.10	
Xuan Jiang	0.03	
FTE Equivalent:	0.66	
Total Number:	12	

Names of Post Doctorates

<u>NAME</u>	<u>PERCENT SUPPORTED</u>
Christian Doonan	0.22
Rahul Banerjee	0.22
Qianrong Fang	0.22
Seong Kyun Kim	0.20
Adam Duong	0.15
Zheng Lu	0.15
Sungjun Hong	0.07
Dani Peri	0.05
Siddhartha Das	0.05
Hexiang Deng	0.05
Shun Wan	0.05
Thomas Glover	0.05
Hiroyasu Furukawa	0.03
Ho Yong Lee	0.50
Andras Olasz	0.20
Jiyoung Jung	0.50
Xinli Song	0.10
FTE Equivalent:	2.81
Total Number:	17

Names of Faculty Supported

<u>NAME</u>	<u>PERCENT SUPPORTED</u>	National Academy Member
Omar Yaghi	0.02	
Dongwhan Lee	0.02	
FTE Equivalent:	0.04	
Total Number:	2	

Names of Under Graduate students supported

<u>NAME</u>	<u>PERCENT SUPPORTED</u>
FTE Equivalent:	
Total Number:	

Student Metrics

This section only applies to graduating undergraduates supported by this agreement in this reporting period

- The number of undergraduates funded by this agreement who graduated during this period: 0.00
- The number of undergraduates funded by this agreement who graduated during this period with a degree in science, mathematics, engineering, or technology fields:..... 0.00
- The number of undergraduates funded by your agreement who graduated during this period and will continue to pursue a graduate or Ph.D. degree in science, mathematics, engineering, or technology fields:..... 0.00
- Number of graduating undergraduates who achieved a 3.5 GPA to 4.0 (4.0 max scale):..... 0.00
- Number of graduating undergraduates funded by a DoD funded Center of Excellence grant for Education, Research and Engineering:..... 0.00
- The number of undergraduates funded by your agreement who graduated during this period and intend to work for the Department of Defense 0.00
- The number of undergraduates funded by your agreement who graduated during this period and will receive scholarships or fellowships for further studies in science, mathematics, engineering or technology fields: 0.00

Names of Personnel receiving masters degrees

<u>NAME</u> Guannan Liu Jason Fortier Total Number:	 2
---	----------------------

Names of personnel receiving PHDs

<u>NAME</u> Joseph Hunt Qiaowei Li William Morris Anh Phan Justin Riddle Xuan Jiang Wenjun Liu Elizabeth Opsitnick Total Number:	 8
--	--

Names of other research staff

<u>NAME</u>	<u>PERCENT_SUPPORTED</u>
Chain Lee	0.15
Alex Capecelatro	0.02
Ryan Knight	0.02
FTE Equivalent:	0.19
Total Number:	3

Sub Contractors (DD882)

Inventions (DD882)

Scientific Progress

See Attachment (in PDF).

Technology Transfer

FINAL REPORT

August 1, 2007 – October 31, 2012

Selective Capture of CWAs and Containment of Their Neutralization Byproducts by Porous Frameworks Presenting Self-Amplifying and Self-Regulating Reactivities

Submitted by: Dongwhan Lee

PI: Dongwhan Lee
Department of Chemistry, Indiana University
800 E. Kirkwood Avenue, Bloomington, IN 47401
Telephone: (812) 855-9364
Email: dongwhan@indiana.edu

co-PI: Omar Yaghi
Department of Chemistry, UC Berkeley
602 Latimer Hall, Berkeley, CA 94720
Telephone: (510) 643-5507
Email: yaghi@berkeley.edu

February 4, 2013

Project Number: W911NF-07-1-0533
Capability Area: Protection Hazard Mitigation
Period of Performance: August 1, 2007 – October 31, 2012

1. OVERVIEW

- a. This project is focused on the preparation and study of ordered porous materials that are designed to display self-propagating and self-regulating reactivities toward chemical warfare agents (CWAs). Our research objective is to use *functionalizable* porous materials that can be activated in a non-linear fashion to supply a high concentration of neutralizing agents against entrapped OP-based nerve agents. Development of new chemically robust covalent organic frameworks (COFs), metal-organic frameworks (MOFs), and electrically active nanoporous polymer networks complements such efforts by significantly expanding the scope of reaction chemistry within confined spaces. New design principles emerging from studies on such functional group-rich porous materials directly address DTRA/ARO's interests in basic research to counter chemical threats.
- b. In the area of functionalized COFs and MOFs, we focused on the development of new porous materials that are (a) molecularly constructed, (b) maintain large cavity and high surface area, and (c) *post-synthetically* modified through selective and high-yielding chemical transformations. COFs and MOFs with rigid, permanently porous structures have been shown to adsorb a variety of gases. These materials have high surface area and free volume, as well as controllable functionality and metrics; however, little is known about the capacity of these crystalline porous solids for toxic gas adsorption properties. We thus designed and synthesized crystalline materials with reactive sites to study adsorption behaviors of various gases and CWA/simulants.

Specifically, we prepared COF-202 having hydrolytically robust borosilicate linkages (B-O-Si), and demonstrated its good thermal and moisture stability. Zr-MOFs are chemically stable porous solids recently discovered. Considering that porous media need to be used under humid conditions in practical applications, Zr-MOFs are one of the best materials to introduce reactive functionalities for improved ammonia adsorption. First, isoreticular covalent modification of amino-functionalized Zr-MOF was performed. Obtained MOFs have chemical stability, as evidenced by reversible ammonia uptake. More importantly, functionalized Zr-MOFs show greater ammonia uptake capacity than that of pristine MOF. Metallation reactions of novel Zr-MOFs with porphyrin functionality was also carried out. Importantly, the metallated analogues did not lose their high surface area and chemical stability, and demonstrated improved ammonia uptake.

We also designed a MOF that can release stored guest molecules by a controllable external stimulus. Azo-IRMOF-74-III with azobenzene units changes the pore diameter by over 4 Å due to the *trans-to-cis* light-induced configurational change. When propidium iodide dye was loaded into the MOF, the release of the dye from the pores was observed by excitation at $\lambda = 408$ nm; the rate of dye release was diminished when irradiation was stopped. This is the first example of light triggering a response mechanism leading to release of a dye molecule from MOF frameworks.

- c. For self-propagating reaction cascades to detect and neutralized CWAs, we have developed a series of dendritic molecules that spontaneously undergo chain fragmentation reactions upon reaction with fluoride ion (= CWA hydrolysis product). The *reactive modules* to be installed onto the inner surface of COF/MOFs were designed to react with CWAs (or their reaction byproducts) to give rise to a large enhancement in fluorescence intensity (i.e. turn-on) as the signaling event. The quinonemethide (QM) rearrangement reaction, which underpins this reaction chemistry, occurs in a cascade fashion and "runs" along the dendritic molecular backbone. As a consequence, multiple copies of nucleophilic agents are released to covalently capture electrophilic chemical agents. Through a combination of spectroscopic and kinetic studies, we have established structure-dependent changes in the mechanism of chain fragmentation, and obtained the rate constants of this chemically-driven signal transduction. An efficient copper(I)-catalyzed [3 + 2] cycloaddition reaction (= azide-alkyne cycloaddition reaction)

was employed successfully to graft these functional molecules onto alkyl azide-modified glass surfaces (as a model of COF inner surface) without compromising their inherent reactivity.

- d. In parallel with studies on the post-synthetic structural modifications of COF and MOF (see **1b** above), we have explored a series of mesoporous silicates (MPS) SBA-15 with cylindrical pore topology (diameter = 6–9 nm) as a porous and robust structural support to immobilize dendritic reactor/sensor modules (see **1c** above). Building upon our expertise in chemical synthesis and materials assembly, we have investigated (i) programmed reagent release from dendritic agents having multiple branching units; (ii) new chromogenic reporter units having longer-wavelength spectral windows; (iii) surface modification with nucleophilic functional groups to trigger and help maintain chain reactions in response to CWAs. A systematic variation in the TEOS:(RO)₃Si-linker-N₃ ratio in the template synthesis of SBA-15 aided these efforts by providing mesoporous materials with fine control over the surface density of azido groups which function as chemical anchoring sites for CWA detox/sensor modules.
- e. As low-dimensional *structural analogues* of borosilicate-based COFs (see **1b** above), we have designed and prepared conjugated polymers (CPs) from π -extended borasiloxane cage monomers. Our exploratory studies on these molecularly constructed and π -conjugated inorganic/organic hybrid materials have established that anodic polymerization of selected bifunctional borasiloxane cage molecules can proceed under ambient conditions to furnish robust thin-film materials that (i) display high electrical conductivity, (ii) selectively recognize volatile chemicals including toxic amines, and (iii) transduce such recognition events into rapid and reversible colorimetric response that can readily be detected without resorting to elaborate optical devices.

Unlike existing CP sensors that typically rely on adsorption-induced swelling and change in the electrical resistivity of composite materials, our borasiloxane-based CPs exploit reversible bond-forming reactions that are directly coupled to changes in visually detectable signals. The high modularity in our synthetic design has facilitated the generation of a large library of borasiloxane cage molecules having systematically varied conjugation length and backbone substituents, both of which should profoundly impact the structural and optoelectronic properties of the resulting CPs. In order to fully establish the structure–property relationships and to identify key structural and functional parameters for selective detection of CWAs, we have also built controlled gas-flow systems with *in situ* spectroscopy capabilities, and also developed chemiresistor arrays for conductance measurements under ambient conditions.

- f. Key achievements:

1. Design and Synthesis of COFs with High Porosity and Thermal/Hydrolytic Stability: A new robust covalent organic framework (COF-202) constructed from borosilicate linkages (B-O-Si) was designed and synthesized. COF-202 has high porosity and thermal stability.
2. Functional Group-Rich MOFs for Reversible Chemical Reactions: By solid-state ¹⁵N NMR measurements, we have confirmed that Zr-MOF (UiO-66) having amino-group rich internal surface can engage in reversible Brønsted acid–base chemistry to afford a mixture of –NH₂ and –NH₃⁺Cl[–] functionalities (termed UiO-66-A).
3. Postsynthetic Functional Group Transformations: UiO-66-A was post-synthetically modified to furnish a mixture of three functionalities, where the hemiaminal functionality is the majority species in UiO-66-B and aziridine is the majority functionality in UiO-66-C. These newly prepared materials are chemically stable, as evidenced by reversible ammonia uptake and release showing capacities ranging from 134 to 193 cm³/g.

4. *Porphyrin-Containing MOFs for Postsynthetic Metallation*: Two new MOFs (MOF-525 and MOF-545) having porphyrin groups have been synthesized, and structurally characterized. In addition to their large surface areas (BET surface areas of 2620 and 2260 m²/g for MOF-525 and MOF-545, respectively), both MOFs show exceptional chemical stability by maintaining their structures in both aqueous and organic environments.
5. *Postsynthetic Metallation to Prepare Metalloporphyrin-Functionalized MOFs*: MOF-525 and MOF-545 having built-in free ligand units were postsynthetically metallated with iron(III) and copper(II) to yield the corresponding metalloporphyrin-functionalized MOFs without losing their high surface area and chemical stability. Furthermore, the addition of metal ion to the porphyrin unit was shown to considerably enhance the total ammonia adsorption.
6. *Light-Driven Actuation of Azo-Functionalized MOFs as Stimuli-Responsive Porous Materials*: The synthesis and structural characterization of an azobenzene-modified isorecticular MOF (azo-IRMOF-74-III) [Mg₂(C₂₆H₁₆O₆N₂)] were completed. In response to external stimuli (i.e. irradiation with light), this material can release pore-entrapped guest molecules in a reversible fashion.
7. *Single-Trigger, Multiple-Release Reagents*: Taking advantage of covalently-triggered QM rearrangements, we have prepared a series of branched molecules that are designed to undergo controlled chain fragmentation reactions. Upon reaction with fluoride anion (= CWA hydrolysis product), these reagents display fluorescence turn-on response, and release nucleophilic phenoxide ions that covalent capture CWA simulants.
8. *Surface Immobilization of Dendritic Molecules*: Using copper(I)-catalyzed azide-alkyne cycloaddition reactions, we have grafted alkyne-tethered reactive modules onto the surface of azide-modified glasses or MPSs. We have also confirmed that surface immobilized reagents still maintain their reactivity toward F⁻.
9. *Mechanisms of Signal Transduction and Structure-Reactivity Relationships*: We have carried out extensive kinetic studies to reveal a dual mechanism of signal transduction through chain fragmentation reactions. The kinetic parameters obtained from these studies show strong dependence on the chemical structures of the linker groups that connect "masked" nucleophiles.
10. *Functionalizable Mesoporous Silicates*: A series of azido-functionalized MPS materials were prepared and post-synthetically modified with various alkyne-tethered dendritic reagents and fluorogenic reporter molecules. We have demonstrated that a wide range of functional groups can be installed onto the inner surface of MPS, the "surface density" of which could be directly quantified by straightforward spectroscopic analysis of released chromophore reporters.
11. *Inorganic Cage Molecules to Construct π -Conjugated Polymers*: An efficient [2 + 2]-type cyclocondensation reactions furnished bifunctional borasiloxane cage molecules, which could be electropolymerized to form air-stable thin films that respond reversibly to volatile TICs including amine vapors.
12. *Dual Mode of Sensing with Nanoporous Conjugated Polymers*: We have shown that both optical transitions and electrical conductivities of the borasiloxane-based conducting polymers (BCPs) respond sensitively to volatile substrates. This dual mode

of sensing allows for cross-validations, and minimizes false positive sensory signaling.

2. TECHNICAL PROGRESS DURING THE REPORTING PERIOD

a. Reticular Synthesis of Covalent Organic Borosilicate Frameworks: Linking molecular building blocks into extended structures by strong covalent bonds is now commonly practiced in the synthesis of MOFs. We have demonstrated that this chemistry can be extended to the linkage of organic units through covalent bonds to small, main-group elements (C–C, C–B, and B–O) to construct COFs. We further demonstrated the generality of this approach by linking organic units with the strong covalent bonds found in Pyrex (borosilicate glass, B–O and Si–O) to assemble a porous covalent organic borosilicate framework designated as COF-202. The synthesis of crystalline COF-202 was carried out by combining a 1:2 v/v dioxane/toluene solution mixture of *tert*-butylsilane triol, $t\text{BuSi}(\text{OH})_3$, and tetra(4-dihydroxyboryl-phenyl)methane, $\text{C}\{\text{C}_6\text{H}_4[\text{B}(\text{OH})_2]\}_4$, (**A** and **D**, respectively; see Figure 1) in a sealed glass tube. This solution was heated to 120 °C for 3 days to yield a white microcrystalline powder whose composition coincided well with the expected formula of $\text{C}_{107}\text{H}_{120}\text{B}_{12}\text{O}_{24}\text{Si}_8 = [\text{C}(\text{C}_6\text{H}_4)_4]_3[\text{B}_3\text{O}_6(t\text{BuSi})_2]_4$. The structure of COF-202 was confirmed by PXRD (Figure 2A), solid-state ^{11}B , ^{29}Si and ^{13}C NMR spectra.

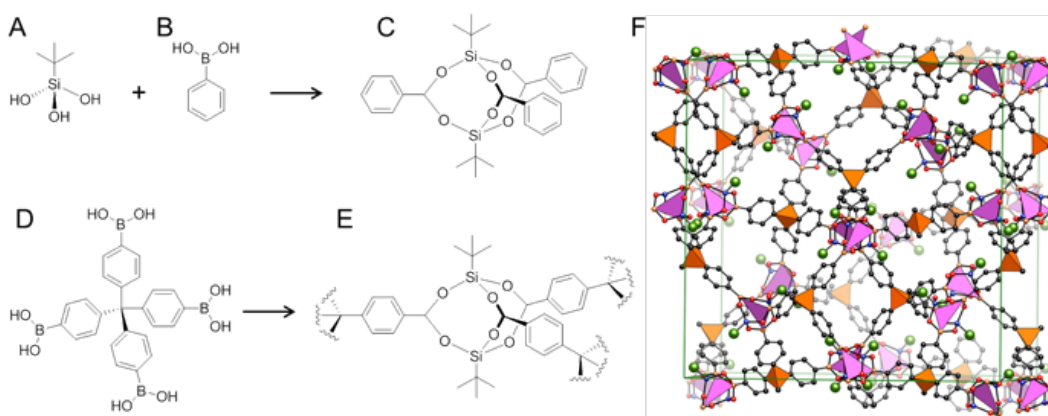


Figure 1. Condensation of *tert*-butylsilane triol **A** with monotopic boric acid **B** forms the molecular borosilicate cage **C**. Condensation of **A** with divergent boric acid **D** leads to the building unit **E** in which the boron atoms occupy the vertices of a triangle and join together the tetrahedral building blocks **D** to give COF-202 **F**. Atom colors: C, black; Si, blue; O, red; B, yellow (H atoms have been omitted and *tert*-butyl groups are represented as green spheres for clarity).

Thermogravimetric analysis showed that COF-202 is stable up to 450 °C, and is insoluble in common organic solvents such as alkanes, tetrahydrofuran (THF), alcohols, acetone, and *N,N*-dimethylformamide (DMF). Moreover, samples of COF-202 maintain good porosity and crystallinity after exposure to air for 24 h. Immersion of COF-202 in anhydrous THF and subsequent evacuation under vacuum at 85 °C for 16 h remove all volatile guests from the pores and activate the material for gas adsorption experiments. The porosity of COF-202 was measured by running an argon low pressure isotherm at 87 K (Figure 2B). The observed Type I isotherm indicates that COF-202 is a microporous material. Furthermore, BET and Langmuir models yielded high surface area values of 2690 and 3210 m²/g, respectively.

b. Postsynthetic Modification of Zr-MOF for Ammonia Uptake: Postsynthetic modification of porous MOFs has allowed organic, metal-coordination, and organometallic reactions to be carried out on covalently linked organic functionalities within the pores. However, challenges arise during attempts to characterize the starting points, intermediates, and products of these reactions. We have demonstrated the use of solid-state ^{15}N NMR spectroscopy to elucidate the

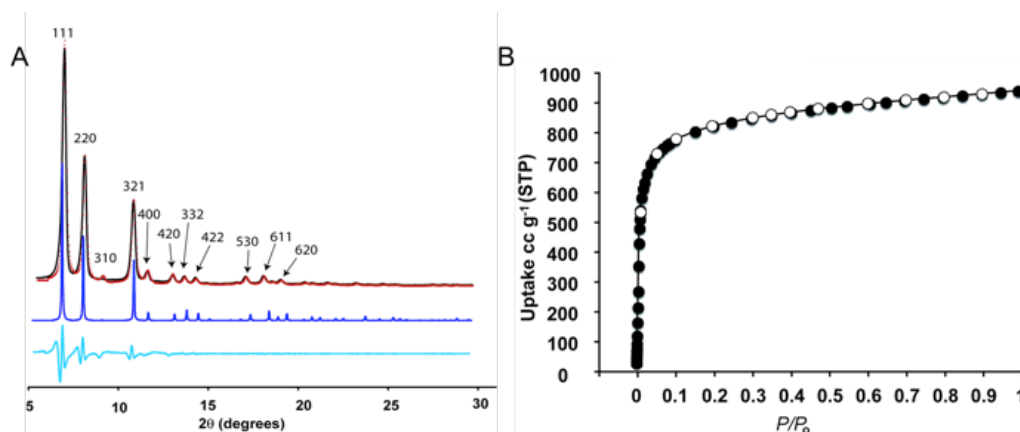


Figure 2. (A) Experimental (black) and calculated (blue) PXRD patterns for COF-202 including Le Bail fitting (red) and the difference plot (light blue). (B) Ar isotherm for COF-202 measured at 87 K. Open and filled circles represent adsorption and desorption branches, respectively.

genuine chemical nature of what was presumed to be an amino-functionalized MOF. Specifically, UiO-66 is a zirconium MOF, $[\text{Zr}_6\text{O}_4(\text{OH})_4(\text{BDC})_6]$ (where BDC = 1,4-benzenedicarboxylate), which was recently reported to have an exceptionally high chemical stability. The amino-functionalized UiO-66-NH₂ (hereafter UiO-66-A, Figure 3A) derivative was also prepared and found to have the same topology.

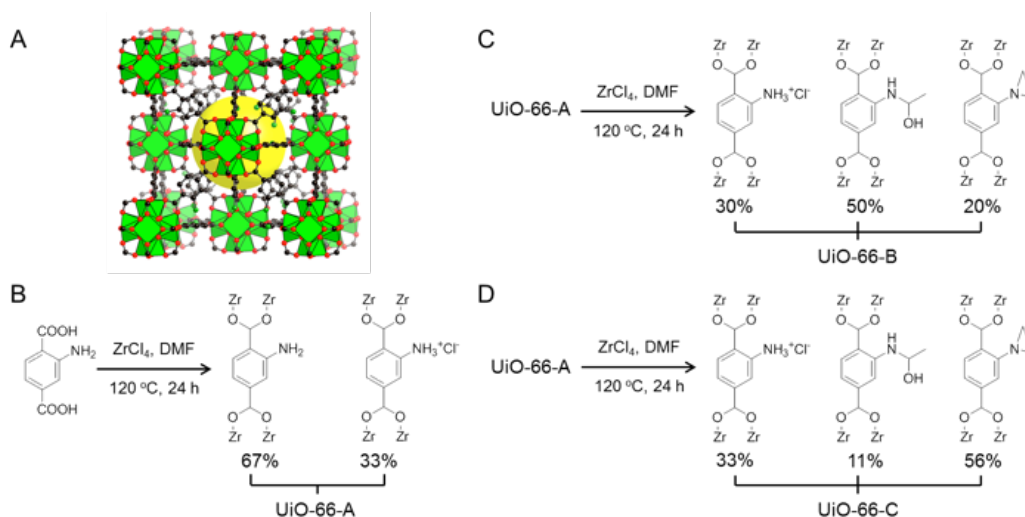


Figure 3. Crystal structure of UiO-66-A. Pores in the evacuated crystalline frameworks are illustrated by yellow spheres that contact the van der Waals radii of the framework atoms. Atom colors: Zr, green polyhedra; C, black; N, green; O, red. (B-D) Synthesis and postmodification of UiO-66-A.

UiO-66-A was synthesized by adding solution mixtures of zirconium tetrachloride in DMF and H₂BDC-NH₂ in DMF. Each of the mixtures was heated to 85 °C and sonicated to dissolve the respective components. The solutions were then combined in a 60 mL scintillation vial and heated to 120 °C for 24 h. The resulting white crystalline powder was collected by filtration. All guest molecules were removed from the pores of UiO-66-A. PXRD analyses were performed on samples of UiO-66-A to ascertain its crystallinity (Figure 4A).

UiO-66-A was further characterized by cross-polarization magic-angle-spinning (CP/MAS) NMR spectra. The ¹⁵N NMR spectrum for UiO-66-A that had been synthesized from ¹⁵N-enriched

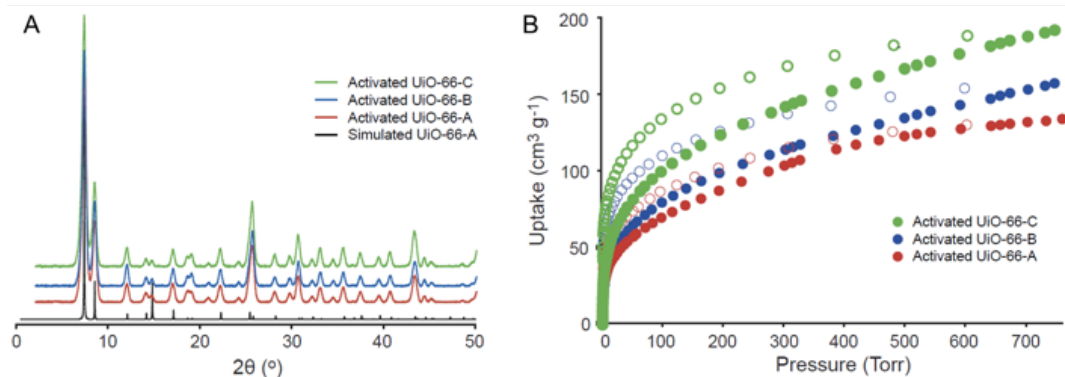


Figure 4. (A) PXRD patterns of UiO-66-A and postmodified compounds (UiO-66-B and -C). Simulated PXRD pattern for UiO-66-A was overlaid. (B) NH_3 isotherm at 298 K of UiO-66-A and postsynthetically modified compounds (UiO-66-B and UiO-66-C).

$\text{H}_2\text{BDC-NH}_2$ showed two resonances at 56 and 137 ppm; these features can be attributed to the free aromatic amine resonance and the protonated amine salt $-\text{NH}_3^+\text{Cl}^-$, respectively. Given that hydrolysis of ZrCl_4 produces HCl, it is anticipated that the $\text{BDC-NH}_3^+\text{Cl}^-$ salt moiety is produced during MOF formation. Integration of direct-excitation NMR gave an approximate ratio of 2:1 (1.94:1) of the amine, which is in line with results from solution NMR and elemental analysis, i.e., $\text{Zr}_6\text{O}_4(\text{OH})_4(\text{BDC-NH}_2)_4(\text{BDC-NH}_3^+\text{Cl}^-)_2$. Prior to carrying out reactions on UiO-66-A, its porosity was assessed by measuring the N_2 gas adsorption isotherm at 77 K (BET surface area = $820 \text{ m}^2/\text{g}$).

A common reaction in molecular organic chemistry is the condensation reaction of an aldehyde and an amine to form an imine moiety. We thus prepared UiO-66-B by adding CH_3CHO to UiO-66-A in CHCl_3 . The solid-state ^{15}N NMR spectrum of UiO-66-B did not show the expected imine resonances, but instead two new resonances at 93 and 71 ppm were observed. The peak at 93 ppm is attributable to a hemiaminal nitrogen. The MAS ^{13}C NMR spectrum of UiO-66-B synthesized from isotopically labeled $^{13}\text{CH}_3^{13}\text{CHO}$ supports the assignment, displaying resonance peaks at 85 and 49 ppm due to the secondary and primary carbon atoms of the hemiaminal, respectively. The additional peak at 71 ppm in the ^{15}N NMR spectrum is consistent with the presence of an aziridine ring, which is also supported by the isotopically enriched ^{13}C MAS NMR spectrum in the resonance at 20 ppm. Integration of a direct-excitation NMR spectrum gave approximate yields of each reaction with 3:5:2 (1:1.74:0.72) of the protonated amine, hemiaminal, and aziridine, respectively.

The putative mixture of functional groups led us to hypothesize that both the kinetic (hemiaminal) and the thermodynamic (aziridine) products were present within the pores of UiO-66-C. Thus, we heated samples of UiO-66-B to 100°C for 12 h to ascertain whether the yield of the thermodynamic product could be increased. Indeed, after heating, samples of UiO-66-B changed from yellow to bright green. ^{15}N NMR spectra obtained from a sample of thermally treated UiO-66-C showed a decrease in the intensity of the hemiaminal product peak at 93 ppm and an increased intensity of the aziridine peak at 71 ppm. The isotopically enriched ^{13}C NMR spectrum showed an analogous relationship between the hemiaminal and aziridine resonances, further confirming the ^{15}N assignments. Again, to quantify the transformation, direct excitation of the ^{15}N NMR spectrum showed a ratio of 3:1:5 (1:0.28:1.68) for the protonated amine/hemiaminal/aziridine.

To confirm that the structure was maintained during the postsynthetic modification reactions, PXRD peaks were examined: both UiO-66-B and UiO-66-C maintained their crystallinity and structure (Figure 4A). Furthermore, the N_2 adsorption isotherm at 77 K demonstrated that UiO-66-B and UiO-66-C retained porosity with BET surface areas of 780 and $800 \text{ m}^2/\text{g}$, respectively. The exceptional stability and unique functionality of these frameworks provide excellent oppor-

tunities to explore the adsorption chemistry of gas molecules such as NH_3 , previously considered to be too reactive for MOFs. Ammonia isotherms were thus obtained at 298 K for the three compounds (Figure 4B), and found to have significant uptake capacities at 760 Torr ($134 \text{ cm}^3/\text{g}$, UiO-66-A; $159 \text{ cm}^3/\text{g}$, UiO-66-B; $193 \text{ cm}^3/\text{g}$, UiO-66-C). Although this value is lower than the uptake observed for MOF-5 ($270 \text{ cm}^3/\text{g}$ at 760 Torr), the stability of UiO-66-A-C materials, as evidenced by maintenance of the analogous structure (NMR) and crystallinity (PXRD), following adsorption and desorption provides important advantages.

c. Synthesis, Structure, and Metalation of Two New Highly Porous Zr-MOFs: Recently, MOFs based on the zirconium(IV) cuboctahedral secondary building unit (SBU), $\text{Zr}_6\text{O}_4(\text{OH})_4(\text{CO}_2)_{12}$ (Figure 5A), and related expanded analogues with ditopic organic struts have been reported. All of these MOFs have a face-centered-cubic (**fcc**) topology and high thermal and chemical stability. Thus far, no other topologies have been reported for this important class of zirconium-based MOFs. We thus explored this chemistry further to establish that this 12-connected SBU (Figure 5A) can be linked with the deprotonated form of the 4-connected links (Figure 5B), tetracarboxyphenylporphyrin ($\text{H}_4\text{-TCPP-H}_2$), to form 3D MOFs (MOF-525), which has a **ftw** topology (Figure 5C,D). We also demonstrated how this SBU can be deployed as an 8-connector SBU (Figure 5E) by blocking four coordination sites on the zirconium atoms with water ligands and how linking this SBU with TCPP can form a MOF structure (MOF-545) with a **csq** topology (Figure 5F,G).

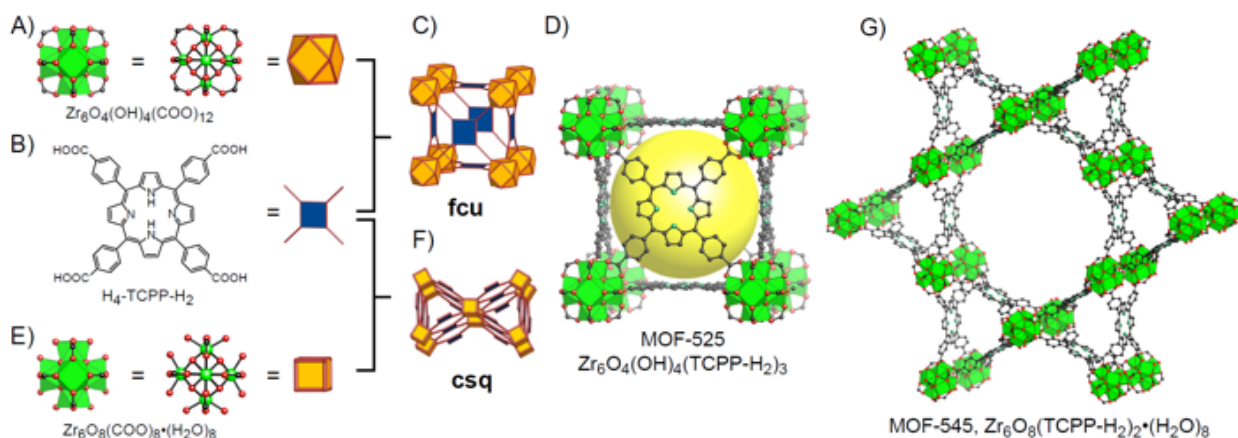


Figure 5. Crystal structures of MOF-525 and MOF-545: (A) cube octahedral unit, $\text{Zr}_6\text{O}_4(\text{OH})_4(\text{CO}_2)_{12}$; (B) porphyrin linker used in MOF-525 and -545 [$\text{H}_4\text{-TCPP-H}_2$]; (C) **ftw** topology; (D) MOF-525; (E) cube unit, $\text{Zr}_6\text{O}_8(\text{CO}_2)_8(\text{H}_2\text{O})_8$; (F) **csq** topology; (G) MOF-545. Pores in the frameworks are illustrated by yellow spheres. Atom colors: Zr, green polyhedra; C, black; N, green; O, red. Hydrogen atoms are omitted.

MOF-525 was prepared as follows: zirconyl chloride octahydrate was added to DMF and sonicated for 30 min. Following sonication, $\text{H}_4\text{-TCPP-H}_2$ was added to the solution. After 10 min further sonication, acetic acid was added to the solution. The solution was placed in a 20 mL scintillation vial and heated at $65 \text{ }^\circ\text{C}$ for 3 days. The microcrystalline powder was filtered and washed with DMF. The DMF was then replaced with acetone, and the volatile acetone was removed by heating at $120 \text{ }^\circ\text{C}$ under vacuum to obtain guest free samples. The structure of MOF-525 was confirmed by PXRD analysis (Figure 6A, Rietveld refinement was performed). MOF-545 was also prepared by a solvothermal reaction, but formic acid was added to a reaction mixture instead of acetic acid. The reaction mixture was heated at $130 \text{ }^\circ\text{C}$ for 3 days to obtain single crystals. For structure determination of MOF-545, MOF-545-Fe crystal with metallated organic linker ($\text{H}_4\text{-TCPPFeCl}$) was used.

To assess the porosity of MOF-525, and -545, Ar adsorption isotherms at 87 K were measured for the guest-free materials (Figures 6B and 7B). The Ar isotherms for each MOF clearly

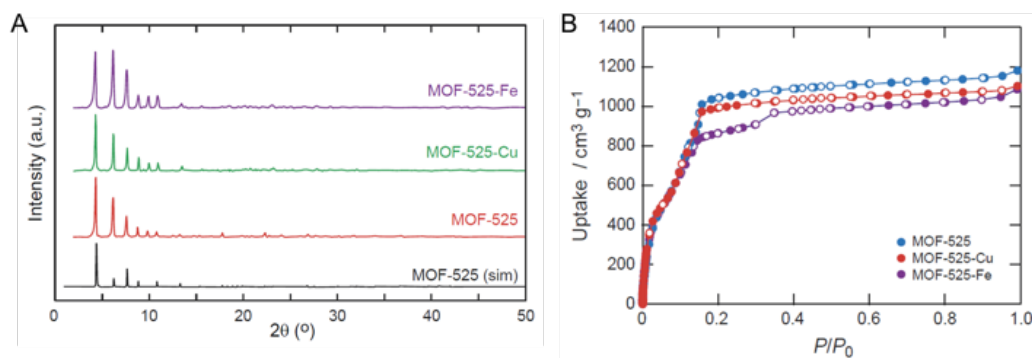


Figure 6. (A) PXRD patterns of MOF-525 and its metalated version. Simulated PXRD pattern for MOF-525 was overlaid. (B) Ar isotherms of MOF-525 and its metalated version measured at $T = 87$ K.

showed a reversible argon adsorption indicative of permanent porosity. Surface area analysis of MOF-525 and MOF-545 by the BET method gave surface areas of 2620, and 2260 m^2/g , respectively. MOF-525 has the highest surface area reported for a zirconium-based MOF. The step position observed in the argon isotherm of MOF-545 supports the mesoporous size of the large hexagonal pore. The chemical stability of MOF-525 and MOF-545 was evaluated by immersing the activated structures in methanol, water, and acidic conditions (water:acetic acid = 50:50, v/v) for 12 h (Figure 7A). Upon reactivation of these MOFs by immersion into acetone followed by evacuation at 30 mTorr, the crystallinity and porosity of the materials were completely recovered.

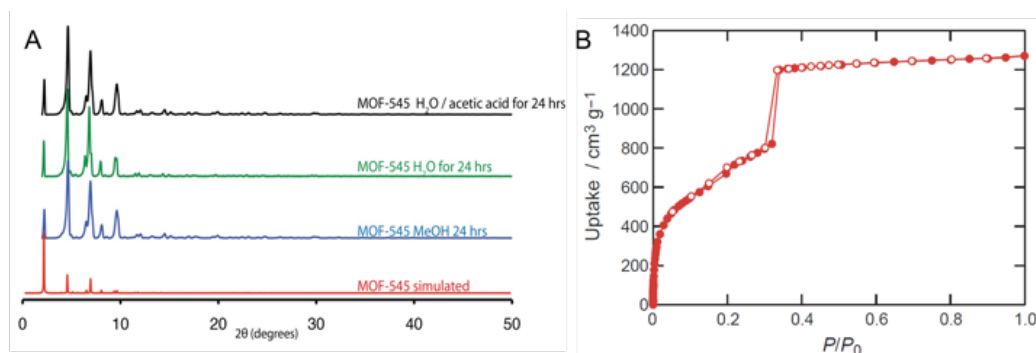


Figure 7. (A) PXRD patterns of MOF-545 after the stability tests. Simulated PXRD pattern for MOF-545 was overlaid. (B) Ar isotherms of MOF-545 measured at $T = 87$ K.

The incorporation of active metal sites into MOF materials should be important to enhance their gas adsorption properties. Both porphyrin-containing MOFs (MOF-525 and MOF-545) have high porosity, chemical stability, and accessible porphyrin sites. Therefore, two methods were employed to obtain metallated porphyrins: pre-assembly and post-assembly metallation. Specifically, pre-assembly metallation was achieved using $\text{H}_4\text{-TCPP-Cu}$ and $\text{H}_4\text{-TCPP-FeCl}$ under synthetic conditions similar to those of MOF-525 and MOF-545 to form MOF-525-Cu [$\text{Zr}_6\text{O}_4(\text{OH})_4(\text{TCPP-Cu})_3$], MOF-545-Fe [$\text{Zr}_6\text{O}_8(\text{TCPPFeCl})_2(\text{H}_2\text{O})_8$], and MOF-545-Cu [$\text{Zr}_6\text{O}_8(\text{TCPPCu})_2(\text{H}_2\text{O})_8$]. Pre-assembly metallation was not successful for isolation of a pure iron analogue of MOF-525 with $\text{H}_4\text{-TCPP-FeCl}$. Therefore, post-assembly metallation of the open porphyrin sites of MOF-525 was used to quantitatively introduce iron(II) atoms into the porphyrin sites of MOF-525. To achieve this, iron chloride was dissolved in DMF and MOF-525 was added to the solution and heated to 100 $^\circ\text{C}$ for 12 h. Unreacted metal salts and DMF were removed by activation conditions analogous to those of MOF-525.

Analysis of the PXRD patterns showed that the metallated derivatives of MOF-525 and MOF-545 have the same structures as their non-metallated analogues. Analysis of the nitrogen isotherms of each MOF revealed BET surface areas comparable to those of the non-metallated analogues. To confirm that each MOF was quantitatively metallated, the samples were digested in 2 M NaOH, and UV-vis spectroscopy study was performed; in no case was free porphyrin observed in the digested material.

We decided to investigate the ammonia adsorption in these frameworks (Figure 8). At 298 K, MOF-525-Fe showed the highest uptake of ammonia reported for a Zr-based MOF. Furthermore, the addition of metal to the porphyrin unit was shown to considerably enhance the total ammonia adsorption. Interestingly in MOF-525 and the metallated analogue, a step was observed in the ammonia isotherm, which can be attributed to the adsorption of a second layer of adsorption within the porphyrin containing MOF; the position of this step is altered by the addition of the metal.

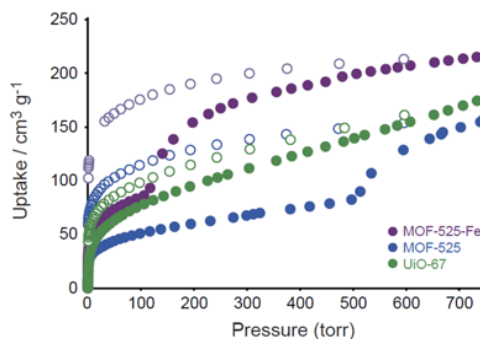


Figure 8. (A) NH_3 isotherm at 298 K of MOF-525 and MOF-525-Fe. As a reference, the NH_3 isotherm for UiO-67 was overlaid.

d. Photophysical Pore Control of an Azobenzene-Containing MOF: MOFs are highly porous and typically exhibit large surface areas. However, to date, the storage and release of guest molecules has relied solely on the uncontrolled diffusion of cargo into and out of the extended structures of the MOFs. Although many MOFs have been synthesized, none have demonstrated on-command release of stored guest molecules using controllable external stimuli. We thus implemented the synthesis and photoisomerization studies of a non-interpenetrated azobenzene-derivatized MOF, azo-IRMOF-74-III (Figure 9), which contains 1-D pores. In this particular MOF, the size and shape of the apertures are controlled by the conformational changes in the azobenzenes, which can be reversibly switched from *trans* to *cis*, or from *cis* to *trans* using UV or visible irradiation, respectively. When all of the azobenzene units are in the *trans*-conformation the pore apertures are 8.3 Å in diameter, but upon switching to the *cis*-conformation, the size of the aperture is increased significantly.

Azo-IRMOF-74-III was prepared by combining $\text{Mg}(\text{NO}_3)_2 \cdot 6\text{H}_2\text{O}$ and the azobenzene-functionalized linker in a solution of DMF, EtOH and H_2O for 24 h at 120 °C. After 24 h, the red

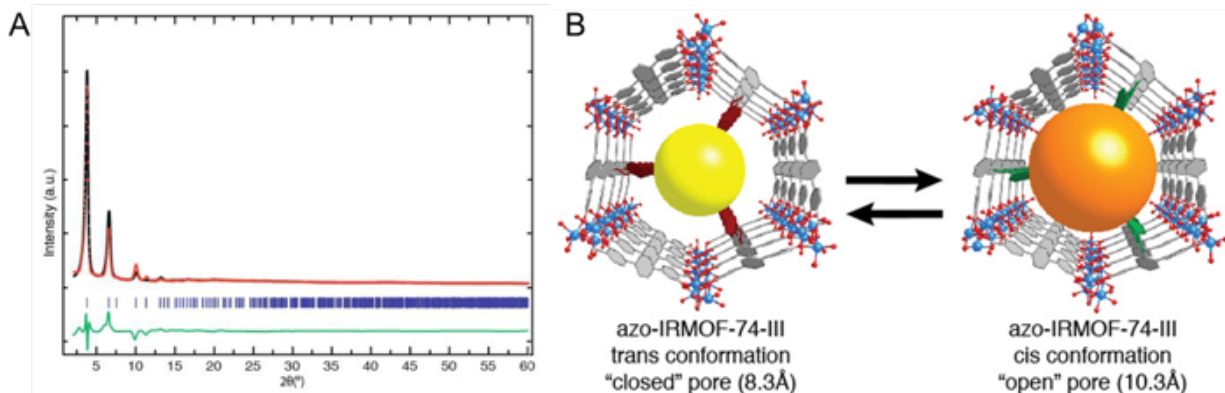
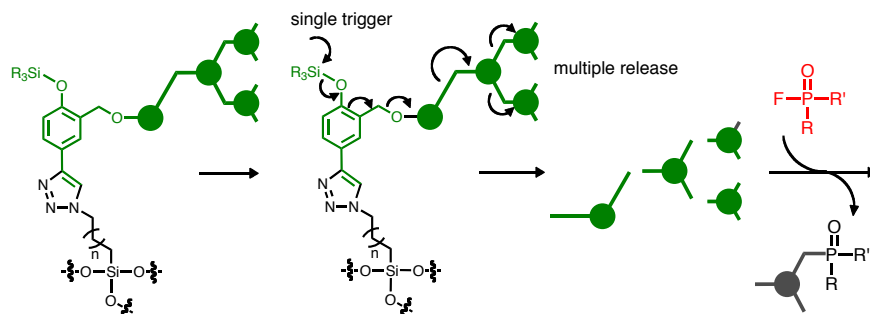


Figure 9. ((A) Experimental (red) and refined (black) PXRD patterns of azo-IRMOF-74-III after Rietveld refinement. The difference plot is indicated in green. Blue ticks indicate the positions of Bragg reflections. (B) Viewing azo-IRMOF-74-III down the *c*-axis displays one-dimensional pores and azobenzene functional groups projecting into the pores. The yellow and orange balls represent pore aperture in azo-IRMOF-74-III, when the azobenzene functional groups are in *trans* and *cis* conformation, respectively.



Scheme 2. Controlled chain fragmentation and release of nucleophilic reagents and sensor modules responding to CWAs.

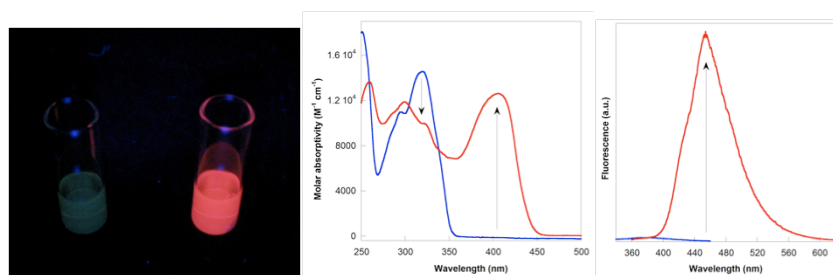
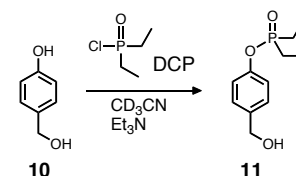


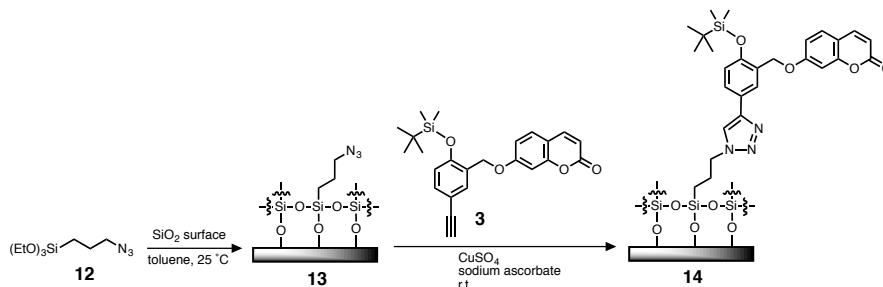
Figure 11. (a) Digital images of **1** in THF illuminated with a hand-held UV lamp ($\lambda = 254$ nm) prior to (left) and after (right) addition of F^- . (b) Changes in the UV-vis (left) and fluorescence (right) spectra of **3** in THF prior to (blue) and after (red) addition of F^- (10 equiv, delivered as Bu_4NF salt), $T = 298$ K.

detox/detection cycle, however, the chain fragmentation product, i.e. 2- or 4-hydroxybenzyl alcohol, should directly react with CWAs to produce F^- so that the cleavage–rearrangement–release cascade (Scheme 2) propagates to other modules until all the COF-entrapped CWAs are neutralized. In order to validate this proposal, a model reaction between 4-hydroxybenzyl alcohol (**10**; chain fragmentation reaction product) and diethylchlorophosphate (DCP; CWA simulatant) in CD_3CN was monitored by ^{31}P -NMR (Scheme 3). We have confirmed that the deprotonated **10**, generated in situ by treatment with Et_3N , reacted quantitatively with DCP ($\delta = +5.0$ ppm, ^{31}P -NMR) under ambient conditions to furnish the corresponding phosphate adduct **11**, which was identified by its characteristic ^{31}P -NMR resonance at -4.8 ppm. Control experiments fully established the requirement of **10** in DCP decomposition.



Scheme 3. Model studies of CWA neutralization (using DCP as simulatant) by the chain fragmentation reaction product **10**.

g. Immobilization of Reactive Modules on Silicate Surface: Modeling the Reaction Environment of the COF Inner Surface: In order to test the feasibility of functionalizing COF inner surfaces with azide–alkyne cycloaddition reactions, we have immobilized **3** (Scheme 1) onto glass surfaces and tested its reactivity toward F^- . As shown in Scheme 4, an azido-functionalized surface was prepared by reaction between pre-cleaned cover glass with 3-azidopropyl triethoxysilane (**12**) using standard silanization protocols. Contact angle measurements confirmed increased hydrophobicity of the modified surface (**13**). Copper-catalyzed Huisgen [3 + 2] dipolar cycloaddition of **3** onto **13** proceeded cleanly under ambient conditions to furnish covalently-modified glass surface (**14**) presenting “masked” reagent modules derived from **3**. Reactivity studies fully established that the surface-bound reagent responds to F^- to release the fluorogenic reporter.



Scheme 4. Covalent modification COF model surface by copper-catalyzed Huisgen [3+2] cycloaddition.

h. Mechanistic Understanding of Chain Fragmentation: Structure–Reactivity Relationships in Quinonemethide Rearrangement: The chain fragmentation shown in Scheme 2 proceeds via QM intermediates which rapidly undergo rearrangement reactions to release the leaving groups in a cascade manner. Despite the importance of QM in many biological processes and its increasing popularity in synthetic pro-drug delivery systems, no kinetic studies were available that directly determined the rate of QM rearrangement and correlated it to the nature of leaving/spacer groups. The release of multiple copies of neutralizing agents and reporter units in our proposed system (Figure 12) relies critically on the efficiency of QM rearrangement, which is directly coupled the response kinetics of smart COFs as first line of defense against CWAs (Figure 13).

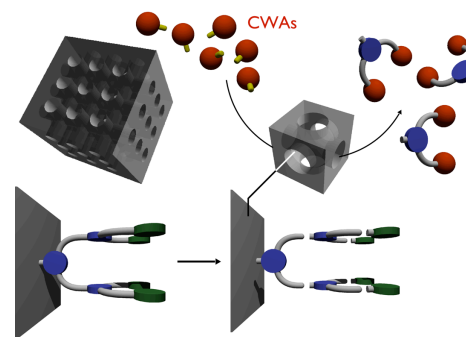


Figure 12. A schematic diagram of an “idealized” COF system with *CWA-responsive reactive modules* anchored onto the the inner surface of large and non-collapsible cavities.

In order to aid rational structure design of such reactive modules, we have extensively studied the response kinetics of the compounds **4** and **8** (Scheme 1), and **15–18** (Scheme 5). Installation of the turn-on fluorescence reporter umbelliferon (**19**; see Figure 14) was ideal for measuring directly the QM rearrangement rates. We focused on the fragmentation kinetics of (i) ether vs carbonate linker, i.e. **4** vs **8**, and (ii) *ortho*- vs *para*-substitution pattern, i.e. **15** vs **17**; **16** vs **18**.

In THF, **8** instantaneously reacted with F^- to release **19**, whereas **4** showed significantly slower response despite that the Si–O bond cleave step in both cases should proceed with similar rate constants (Figure 14). A careful analysis using the kinetic models shown in Figure 14 clearly indicated a strong dependence of response kinetics on the nature of the leaving group. Specifically, the carbonate-linked **8**, despite having an additional fragmentation step to release CO_2 , collapsed more rapidly than **4**. Fittings to kinetic traces enabled us to determine the rate constants of Si–O cleavage and QM rearrangement steps for a series of compounds. Comparative studies with models **15–18** further established an essentially identical kinetic be-

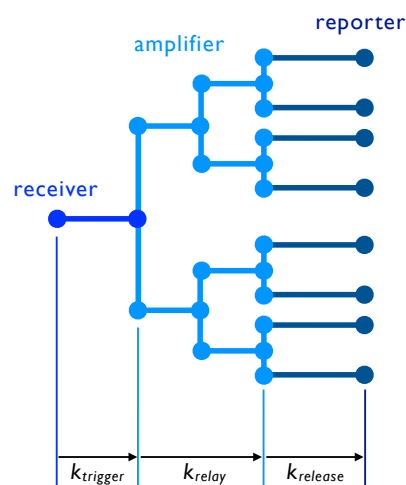
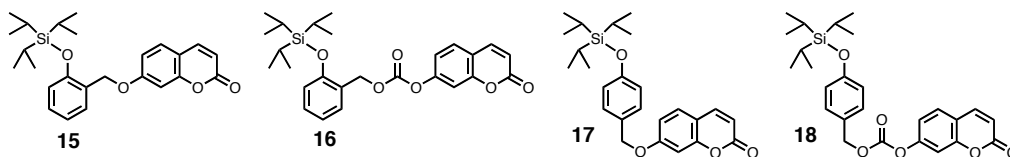


Figure 13. A schematic diagram of a *single-trigger, multiple-release* system, the response rate of which is dictated by the parameters $k_{trigger}$, k_{relay} , and $k_{release}$. A detailed understanding of the structure–reactivity relationship that underpins this cascade event is critical for the rational design of CWA detox system with feedback regulation, programmed signal delay, and timed release capabilities. .



Scheme 5. Chemical structures of model compounds used in the QM rearrangement kinetic studies.

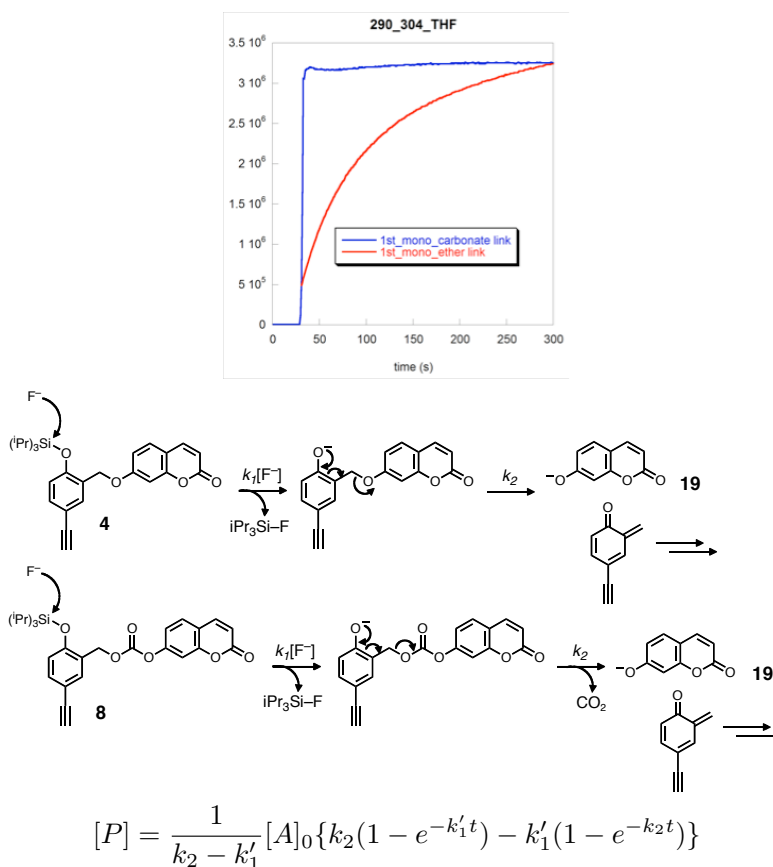
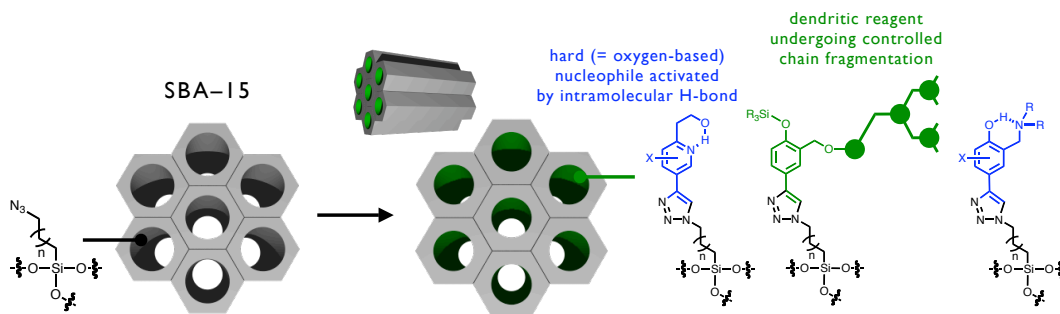


Figure 14. Controlled chain fragmentation of **4** (red) and **8** (blue) in THF, triggered by F^- (10 equiv; delivered as Bu_4NF salt) and monitored by the growth of the fluorescence emission at $\lambda = 455$ nm. The kinetic data can be fitted with a two-step model with rate constants k_1 (for bimolecular reaction with F^- ; determined under *pseudo*-first order conditions) and k_2 (for unimolecular QM rearrangement). $[P]$ = concentration of the fragmentation product **19**; $[A]_0$ = initial concentration of the reactant, either **4** or **8**; $k_1' = k_1[F^-]$, observed rate constant under *pseudo*-first order conditions, i.e. $[F^-]_0 \gg [A]_0$.

havior regardless of the *ortho*- or *para*-substitution pattern, thereby validating our initial proposal to realize “single trigger and multiple release” schemes with branch-structured reagents responding to CWAs.

i. Preparation of “Functionalizable” Mesoporous Silicates (MPSs) and Post-Synthetic Modifications: In order to implement the ideas outlined in Scheme 6, we have prepared an expanded set of SBA-15- N_3 -X, in which X (= 1, 2, 4, 6, and 8) represents the percent (%) of $(EtO)_3Si(CH_2)_3N_3$ used in the template-assisted co-condensation with $(EtO)_4Si$ to prepare the azido-functionalized MPS.

The PXRD data (Figure 15) confirmed that these materials retain good crystallinity; the surface area and the pore size of SBA-15- N_3 -X (X = 1, 2, 4, and 8) were also determined by BET measurements. The average BET surface of 809.523 m^2/g is in reasonable agreement with previ-



Scheme 6. Surface functionalization of mesoporous silicates through post-synthetic modification.

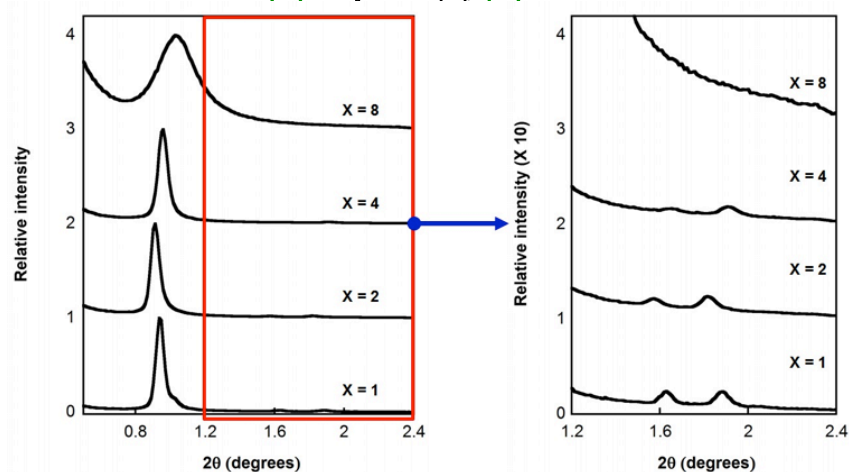
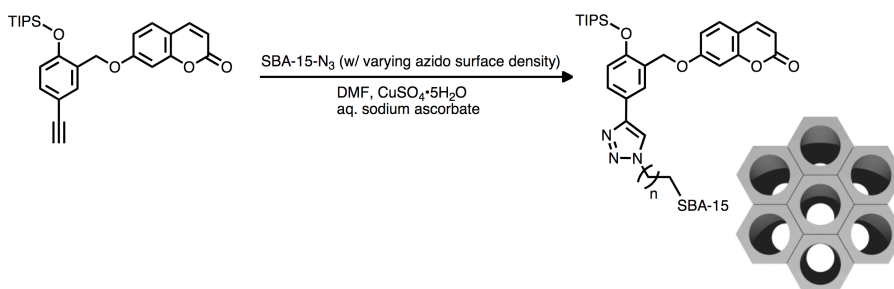


Figure 15. PXRD patterns of SBA-15-N₃-X. (a) The relative intensity was normalized to the (100) diffraction. The patterns were sequentially adjusted by 1.0 intensity units. (b) The patterns were sequentially adjusted by 1.0 intensity units after being multiplied by 10 in order to highlight the (110) and (200) diffractions.

ously reported azido-functionalized SBA-15. In addition, a systematic decrease in pore size (52 Å → 50 Å → 48 Å → 43.6 Å) was observed as the % loading of azidoalkyl precursor is increased.

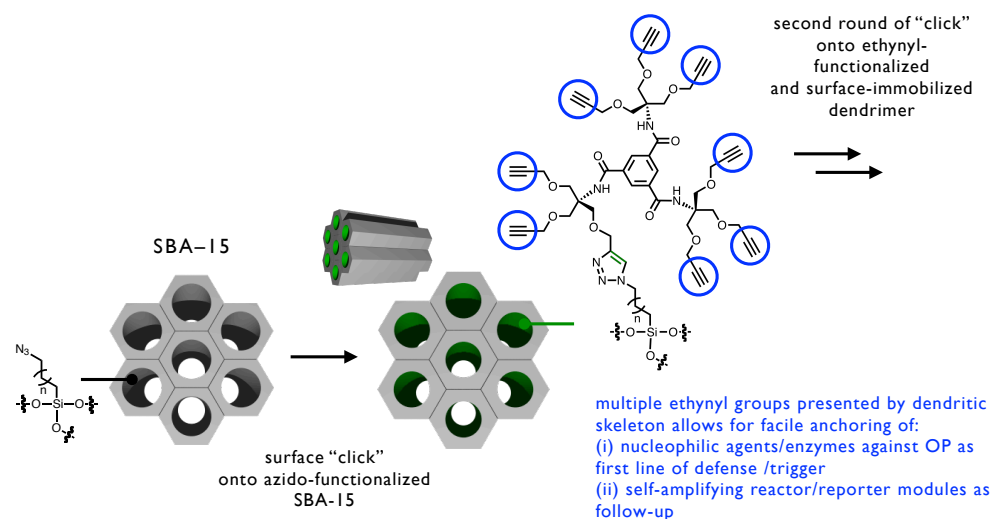
This air-stable and porous material was subsequently reacted with the reporter module (= a structural derivative of **3**) to prepare surface-modified MPS as shown in Scheme 7. Under optimized conditions, fluoride-induced cleavage of the reporter module released 7-hydroxycoumarin as the reporter. Our UV-vis spectroscopic studies established a linear relationship between azide loading and concentration of the reporter group released, which fully establishes that the azide–alkyne cycloaddition reaction proceeds efficiently inside the MPS cavity. In order to map



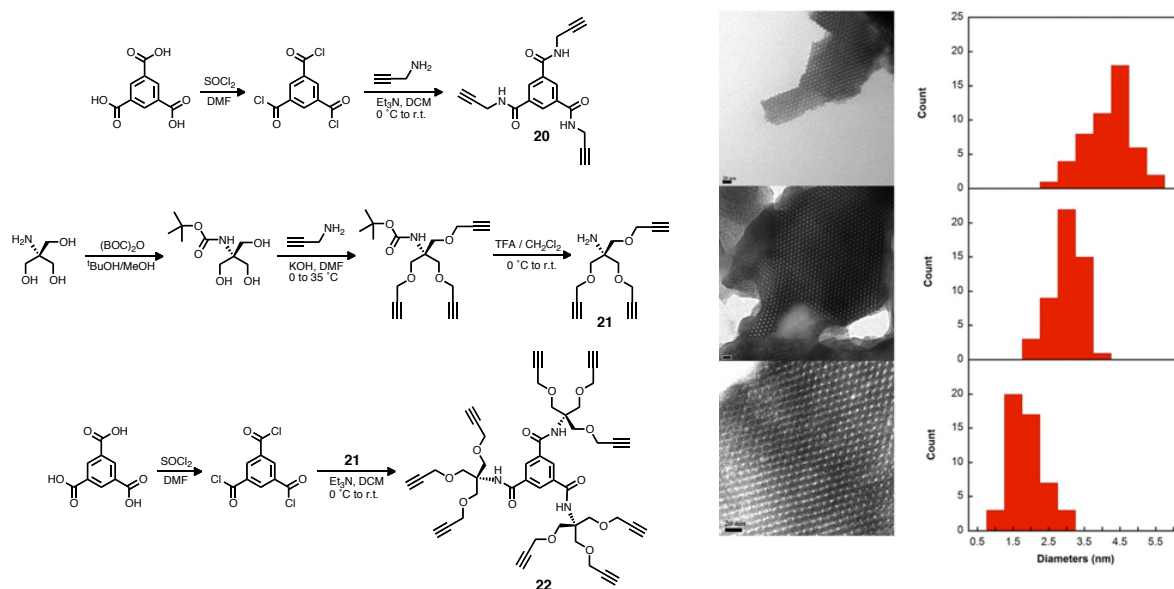
Scheme 7. Surface functionalization of mesoporous silicates through post-synthetic modification.

out the reactive surface of functionalizable MPS, we also carried out “co-click” reactions to simultaneously install reporter and non-reporter molecules in varying ratios. These post-synthetically modified MPS materials were isolated and subjected to standard protocols to release the surface-bound reporter group. UV-vis studies also confirmed that as the ratio of the non-reporter molecule (with respect to the reporter molecule) is increased, the amount of the released reporter is decreased in a linear fashion.

j. Synthesis of Dendritic Scaffolds to Enhance the Surface Density of Reactive Modules: In an effort to increase the surface density of the functional groups to be installed in the inner cavities of MPS, we have carried out the “sequential” click reactions as outlined in Scheme 8. By taking the synthetic routes outlined in Scheme 9, C₃-symmetric dendritic molecules **20** and **22** were prepared. These hyper-branched scaffolds present multiple ethynyl groups for subsequent click reactions with azido-functionalized surfaces and molecules. Using copper(I)-catalyzed cy-



Scheme 8. Sequential click chemistry to introduce hyperbranched functional scaffolds onto the surface of MPS.



Scheme 9. Model studies of CWA neutralization (using DCP as simulant) by the chain fragmentation reaction product **10**.

Figure 16. TEM images of (a) SBA-15-N₃-4, (b) SBA-15-D1st, and (c) SBA-15-D2nd. Histograms showing pore size distributions of (d) SBA-15-N₃-4, (e) SBA-15-D1st, and (f) SBA-15-D2nd.

claddition routes that we have established (see **Section 2i** above), **20** and **22** were grafted onto the azido-functionalized surface of MPS to prepare SBA-15-D1st, and SBA-15-D2nd, respectively. Changes in the pore size of SBA-15-N₃ upon modification with dendrimers were examined by TEM (Figure 16), which showed ordered structures with hexagonal packing, indicating that the click reaction did not affect the morphology of SBA-15. A very narrow size distribution of the pore was also observed across all samples. The average pore size of SBA-15-4-N₃ is ca 42 Å, which nicely correlates with the pore size obtained from BET studies (47 Å). The average pore size of SBA-15-4-D1st, and SBA-15-4-D2nd is 30 and 19 Å, respectively. This systematic change in the pore size distribution is consistent with the increasing molecular dimensions of the dendrimers with increasing generations (Scheme 9).

k. Spectroscopic “Mapping” of Reactive End Groups: For the well-characterized SBA-15-4-D1st, and SBA-15-4-D2nd, we have appended azido-tethered umbelliferone probe molecules by copper(I)-catalyzed click chemistry. The amount of reactive ethynyl groups (i.e. those that are sterically accessible by incoming probe molecules) could be quantified directly by the umbelliferone (= 7-hydroxycoumarin) reporters released by fluoride-induced chain fragmentation (see **Section 2i**).

In addition, a resorufin (=7-hydroxy-3H-phenoxazin-3-one) probe having ethynyl groups could be reacted with the “unreacted” surface azido groups of MPS that had already been functionalized with dendrimers. As shown in Figure 17a, a simultaneous release of umbelliferone and resorufin from MPS was confirmed by the appearance of the absorption peaks at $\lambda = 407$ nm (umbelliferone, $\epsilon = 23,000$ M⁻¹ cm⁻¹) and $\lambda = 571$ nm (resorufin, $\epsilon = 54,000$ M⁻¹ cm⁻¹). The amount of ethynyl group (on the dendrimer) and azide group (on the MPS surface) could be determined directly from the absorbance at $\lambda = 407$ and 571 nm, respectively.

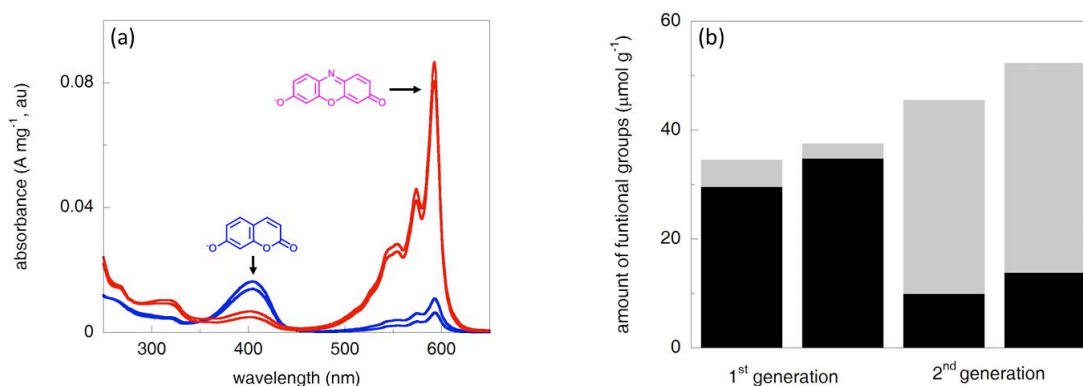


Figure 17. (a) UV–vis spectra of umbelliferone (= 7-hydroxycoumarin) and resorufin (=7-hydroxy-3H-phenoxazin-3-one) released from MPS following cleavage with F⁻ in THF (red, MPS functionalized with 1st-generation dendrimer; blue, MPS functionalized with 2nd-generation dendrimer). (b) The amount of azide (black) and ethynyl (gray) groups determined from the absorbance at $\lambda = 407$ and 571 nm, respectively.

l. New Probe Molecules for Naked-Eye Detection of CWAs: In an effort to develop new colorimetric detection method for CWAs, we prepared an arylazo-based chromophore **23**. Addition of F⁻ to a THF solution of **23** elicited a dramatic color change from yellow to blue, with large spectral shift in absorption peak from $\lambda_{\text{max,abs}} = 441$ to $\lambda_{\text{max,abs}} = 637$ nm (Figure 18). A quinoid-type electronic structure contributes significantly to the broad charge transfer (CT)-type transition of the azo dye fragment **24** released from the trigger–relay–reporter module **23**.

m. Borasiloxane Conjugated Polymer (BCP) as Chemiresistor Sensors: With appropriate steric protection, [2 + 2]-type cyclocondensation reactions between π -conjugated boronic acids and dihydroxysilanes furnish borasiloxane cage molecules (**25**) that can be electropolymerized to form stable thin-film materials of **poly-25** on the electrode surface (Scheme 10). Upon expo-

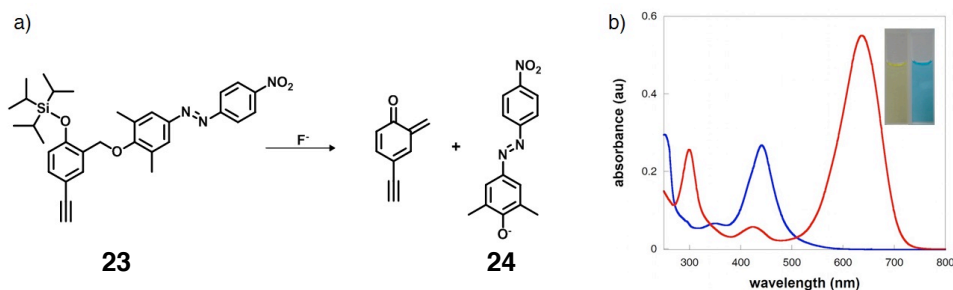
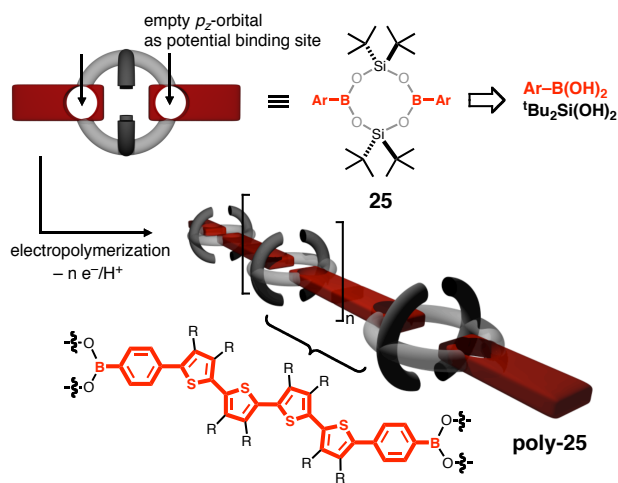


Figure 18. (a) Mechanism of colorimetric response from the reaction between **23** and F^- . (b) Electronic absorption spectra of **23** prior to (blue) and after (red) treatment with fluoride in THF. Inset: photographic images of color change prior to (left) and after (right) addition of F^- .

sure to volatile amine vapors, the dark forest-green color of this partially *p*-doped conducting material immediately turns orange (through a large blue-shift in the polaron/bipolaron transitions from B–N adduct formation), but this color switching could be reversed by treatment with stronger Lewis acid that can scavenge the polymer-entrapped RNH_2 molecules.

In collaboration with Dr. Arthur Snow at Naval Research Laboratory (Washington, D.C.), we have investigated changes in the electrical conductance of BCPs (deposited onto interdigitated microelectrodes) upon exposure to different vapor samples. As shown in Figure 19, the conductivity increased upon exposure to H_2O vapor, but the baseline value was quickly restored after brief purging with N_2 . The *increase in conductivity* as signal read-out is particularly intriguing. In fact, it is a quite rare phenomenon in resistivity-based sensors, which typically undergo *decrease* in conductivity from perturbation of charge conduction pathways. This switching cycle could be repeated multiple times, and the response isotherm shows a nice linear correlation between the conductivity and H_2O vapor pressure. These findings demonstrate that such a device can potentially be used as sensors for both qualitative and quantitative detection of certain vapor samples.

n. Optical Response of BCP Sensors to TICs: In order to gain a quantitative understanding of binding-induced changes in optical properties, we constructed controlled-gas flow systems. Upon a brief exposure to *n*-BuNH₂ vapor (mixing ratio of channel 1/channel 2 = 15%) for 15 s, the transmittance at 525 nm of BCP decreased while the transmittance at 652 nm increased (Figure 20). Purging of this amine-exposed thin film with pure N_2 (for 2 h) restored the initial transmittance, which fully established the reversibility of this process. The relatively long



Scheme 10. Modular synthesis of the borasiloxane cage molecule **25**, and its electropolymerization to **poly-25** as electrode-deposited conductive materials.

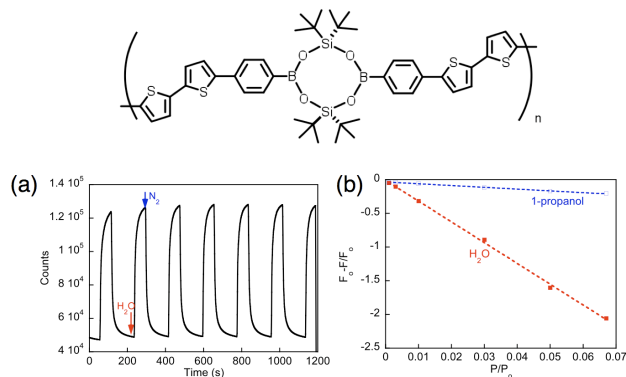


Figure 19. (a) Changes in electrical conductivity upon exposure of CP chemiresistor to H_2O vapor followed by purging with N_2 . (b) Response isotherm to H_2O vs 1-propanol.

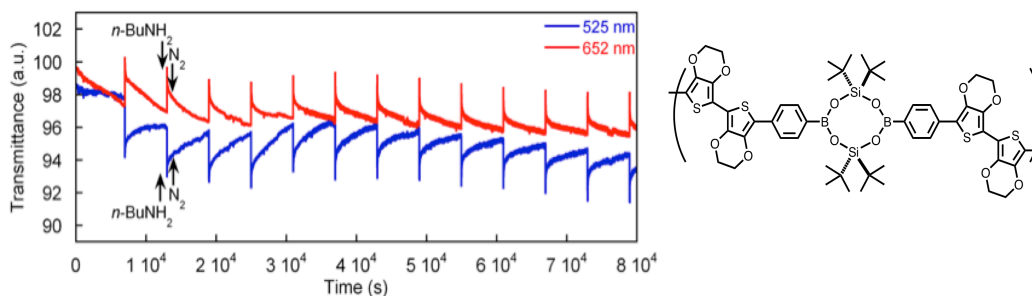
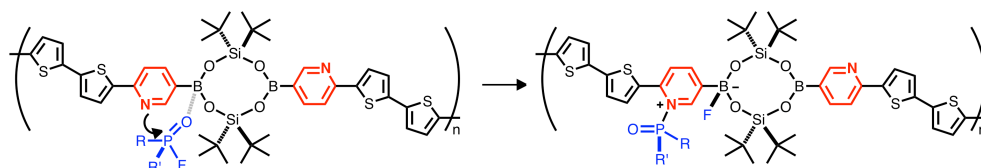


Figure 20. Changes in the transmittance at 652 nm (red) and 525 nm (blue) of a thin film BCP on ITO-coated glass electrode upon exposure to a constant gas flow of 15% (v/v) *n*-BuNH₂-saturated N₂ for 15 s followed by 2 h purge with pure N₂.

purging time required for a full recovery of the baseline is presumably due to the formation of strong Lewis acid–base adduct between the boron center and the amino group. Notably, this sensor showed stable optical change for multiple exposure–purge cycles conducted over a period of 2 days.

We also examined the response of BCP toward different amount of NH₃ by changing the mixing ratio of feeding gases. Despite continuous drop of the baseline, the absolute change in the transmittance (= ΔT) of BCP correlates directly with the concentration of NH₃ applied as gas. This linear dependence of the ΔT on [NH₃] suggests the possibility of using this sensor to quantify the exact concentration of NH₃ or other related toxic TIC/TIM vapors. Importantly, we found that the introduction of humidity does not compromise the sensor performance.

o. Backbone Modification of BCP to Capture Electrophilic CWAs: For nucleophilic capture of OP-based nerve agents, pyridyl functionality was incorporated into borasiloxane monomers. The idea behind this approach is to detoxify OP agents through nucleophilic attack on the phosphoryl group by nitrogen atom on the pyridyl ring. Such a reaction should be promoted by the capture of leaving group, i.e. fluoride ion, by the trivalent boron center to form a stable Lewis acid–base adduct (Scheme 11). The synthesis of target molecule was completed and electro-polymerization under potentiostatic condition (by holding the potential at +1.15 V (vs Ag/Ag⁺) for 10 min) produced BCP as thin film materials deposited directly onto the electrode surface. The pyridine nitrogen atom of the CP retains its basicity even when embedded within the solid matrix. For example, a brief exposure of a thin film of BCP toward HCl vapor in air elicited a visually discernable color change from red to dark orange. The original red color, however, could be fully restored by exposing this acid-treated CP to a saturated vapor of *n*-butylamine. This cycle could be repeated multiple times without noticeable deterioration of the switching performance. We tested the response of BCP to HD simulants including 2-chloroethyl ethyl sulfide and 2-chloroethyl phenyl sulfide. However, no significant spectral shift or color change was observed against HD simulants.



Scheme 11. Double activation and capture of OP agents.

3. SUMMARY AND CONCLUSION

Under the support of DTRA/ARO (W911NF-07-1-0533), we have designed and synthesized highly porous COFs and MOFs as functional architectures that are capable of capturing volatile TICs. In parallel, we have explored novel crystalline porous materials that have reactive sites and functionalities, which can be controlled by an external stimulus. For instance, we demonstrated that reticular chemistry facilitates the design and synthesis of new robust COFs having hydrolytically more robust borosilicate linkages (B–O–Si). With appropriate choice of the substituents on the apical silicon sites, the borosilicate cages could potentially be functionalized to produce hybrid materials. We have also developed reactive sites in chemically stable frameworks through isorecticular covalent functionalization and metallation. The most important conclusion is that the reactive sites in the pore, which interact strongly with guest molecules, are required for ammonia capture. In addition, a MOF with self-contained photo-active switches was prepared to demonstrate the ability to control the release guest molecules from its pores in response to an external stimulus. Our understanding of the synthesis of COFs and MOFs is still in its early stages, but it is clear that functional modification of crystalline porous solids should significantly improve the adsorption capacity of various CWAs and TICs.

As stimuli-responsive functional molecules that can release multiple copies of nucleophilic agents to combat electrophilic CWAs, we have developed linear/branched oligoether/esters. Upon cleavage of a Si–O bond triggered by fluoride anion (= hydrolysis product of OP agent), fast and repetitive QM rearrangement occur along the molecular backbone to release phenoxide derivatives that detoxify OP agent simluant through P–O bond formation. The progress of such reaction could be visually monitored by a large enhancement in the fluorescence intensity, which allows for detection and detoxification achieved by a single integrated molecular system. Through high-yielding click chemistry, we have successfully installed these functional modules onto chemically modified inorganic surfaces including mesoporous silicates. As one-dimensional structural analogue of COF, shape-persistent conducting polymers were also prepared from borasiloxane cage molecules. The light-absorbing properties and electrical conductivities of these air-stable thin film materials change in a reversible fashion upon exposure to volatile TICs including low-molecular weight amines. A chemically-driven signal amplification mechanism that we have developed and refined with these stimuli-responsive molecules should readily be implemented with various structural platforms, including porous matrix of COF and MOF.

4. LIST OF PUBLICATIONS

- [1] Hunt, J. R.; Doonan, C. J.; LeVangie, J. D.; Côté, A. P.; Yaghi, O. M., Reticular Synthesis of Covalent Organic Borosilicate Frameworks. *J. Am. Chem. Soc.* **2008**, *130*, 11872–11873.
- [2] Riddle, J. A.; Jiang, X.; Lee, D. Conformational dynamics for chemical sensing: simplicity and diversity. *Analyst*, **2008**, *133*, 417–422.
- [3] Lee, H. Y.; Jiang, X.; Lee, D. Kinetics of Self-Immolation: Faster Signal Relay over a Longer Linear Distance? *Org. Lett.* **2009**, *11*, 2065–2068.
- [4] Yaghi, O. M.; Li, Q., Reticular chemistry and metal-organic frameworks for clean energy. *MRS bulletin*, **2009**, *34*, 682–690.
- [5] Liu, W.; Pink, M. Lee, D. Conjugated Polymer Sensors Built on π -Extended Borasiloxane Cages. *J. Am. Chem. Soc.* **2009**, *131*, 8703–8707
- [6] Jo, J.; Lee, D. Turn-On Fluorescence Detection of Cyanide in Water: Activation of Latent Fluorophores through Remote Hydrogen Bonds That Mimic Peptide β -Turn Motif. *J. Am. Chem. Soc.* **2009**, *131*, 16283–16291.
- [7] Deng, H.; Olson, M. A.; Stoddart, J. F.; Yaghi, O. M., Robust dynamics. *Nat. Chem.* **2010**, *2*, 439–443.

- [8] Lee, H.; Song, X.; Park, H.; Baik, M.-H.; Lee, D. Torsionally Responsive C_3 -Symmetric Azo Dyes: Azo–Hydrazone Tautomerism, Conformational Switching, and Application for Chemical Sensing. *J. Am. Chem. Soc.* **2010**, *132*, 12133–12144.
- [9] Morris, W.; Doonan, C. J.; Yaghi, O. M., Postsynthetic Modification of a Metal–Organic Framework for Stabilization of a Hemiaminal and Ammonia Uptake. *Inorg. Chem.* **2011**, *50*, 6853–6855.
- [10] Lee, H. Y.; Jo, J.; Park, H.; Lee, D. Ratiometric detection of mercury ion in water: accelerated response kinetics of azo chromophores having ethynyl ligand tethers. *Chem. Commun.* **2011**, *47*, 5515–5517.
- [11] Hutt, J. T.; Jo, J.; Olasz, A.; Chen, C.-H.; Lee, D.; Aron, Z. D. Fluorescence Switching of Imidazo[1,5-a]pyridinium Ions: pH-Sensors with Dual Emission Pathways. *Org. Lett.* **2012**, *14*, 3162–3165.
- [12] Lee, H. Y.; Olasz, A.; Chen, C.-H.; Lee, D. Three-Stage Binary Switching of Azoaromatic Polybase. *Org. Lett.* **2012**, *14*, 6286–6289.
- [13] Jo, J.; Lee, H. Y.; Liu, W.; Olasz, A.; Chen, C.-H.; Lee, D. Reactivity-Based Detection of Copper(II) Ion in Water: Oxidative Cyclization of Azoaromatics as Fluorescence Turn-On Signaling Mechanism. *J. Am. Chem. Soc.* **2012**, *134*, 16000–16007.